First stages of epitaxial growth in the presence of an extended defect: Kinetic Monte Carlo simulations versus rate equation study on a vicinal surface

Florent Dumont,[1] Ali Ramadan,[1,2] Fabien Picaud,[1] Christophe Ramseyer,[1] and Claude Girardet[1]
[1]*Laboratoire de Physique Moléculaire, UMR CNRS 6624, Faculté des Sciences, La Bouloie, Université de Franche-comté, F25030 Besançon Cedex, France*
[2]*Faculté des Sciences et des Technologies Industrielles, Université de Djibouti, Avenue Georges Clémenceau, Boîte Postal 1904 Djibouti Ville, Djibouti*
(Received 4 July 2007; published 19 October 2007)

We study the influence of atom confinement during the growth process on vicinal surfaces with different terrace widths. The behavior of the mean island density n and size s is analyzed in a general way as a function of the flux F over diffusion D_1 ratio and terrace width using kinetic Monte Carlo simulations. We show that the exponent in the scaling law $n \propto (F/D_1)^{\alpha}$ changes from $\alpha=1/3$ for infinite terrace to $\alpha=1$ in the case of finite terrace when the flux is lowered. In the same condition, the island size is limited by confinement, leading to a critical value which depends on the terrace width, only. Very simple rate equations are shown to be able to quantitatively explain, through three parameters determined independently, the simulation results at small deposition flux, whatever the description of the islands (point, compact, or fractal). Application of these results to a physical case Ag/Pt leads to an excellent agreement with more complete simulations based on an atomic description of the growth mechanisms.

DOI: 10.1103/PhysRevB.76.155419 PACS number(s): 64.60.Qb

I. INTRODUCTION

The level of refinement reached by the experimental techniques for probing the epitaxial growth of thin films[1] has stimulated the development of theoretical models to understand the scaling properties of atom distribution on a surface.[2–36] These models are based on probabilistic computational approaches[2–4,14,16,24,27] and on semianalytical methods involving the resolution of a set of deterministic reaction-diffusion equations[5,7,11,13,15,18] which describes the time evolution of average rate coefficients. In fact, most of these theories[10–12,20,21,23] have generally focused on the use of mean-field rate equations as analytic support to Monte Carlo simulations. Kinetic Monte Carlo (KMC) simulations are often considered among the most efficient tools for understanding the complex mechanisms which govern the growth[4,6,23,24] (deposition, diffusion, nucleation, coalescence, desorption, and even incorporation by exchange of particles) on regular templates. Rate equations (RE) approach is a practical way for obtaining semiquantitative scaling laws for the island and monomer densities in the submonolayer regime. In the earliest versions of these methods, homoepitaxial[15,17,18] and heteroepitaxial growths[1,7] were studied on clean surfaces. RE with various approximations to include the capture rates combined with KMC simulations were used to analyze the density and shape of islands on infinite metal surfaces and the results were compared to STM data. The existence of a denuded capture zone around the island was introduced to interpret MC simulations[25,29,30,32–36] in a better way[19] than the mean-field approach. Then, the influence of extended defects such as steps[9,22] and of surfactants[37–40] on the atom diffusion processes, was considered to analyze the formation of self-assembled nanostructures (wires, dots,…) as a function of the deposition flux.

On vicinal surfaces, the step flow growth has been widely considered within the asymmetric barrier step model by Schwoebel-Ehrlich to predict stability and instability in the terrace morphology during epitaxy, in terms of diffusion or transfer equations.[8,41,42] Deposition of atoms onto well-controlled terraces with atomic widths has been much less studied.[43] A reduced set of parameters that intuitively govern the formation of specific morphologies (fractal or compact islands, wires, etc.) on the vicinal surfaces has been tentatively introduced in KMC simulations to define in a predictive way optimum conditions.[44] External parameters (temperature, deposition flux, coverage) were associated to intrinsic parameters characterizing the interactions between adatoms and the steps and between the adatoms themselves to discuss these conditions. However, to our knowledge, no general study on the role of the terrace widths has been performed.

In this paper, we consider the first stages of epitaxial growth of atoms as a function of terrace width using KMC simulations and RE adapted to vicinal surfaces. More particularly, the influence of this width on the monomer diffusion, island formation and size is discussed by varying this width. KMC results are first presented in Sec. II to determine the scaling laws for these quantities as a function of the terrace width within the approximation of relatively small deposition flux of atoms on the surface. Then a simple RE approach is built in Sec. III to calculate mean field quantities by considering that the monomer and island capture can be described through a limited set of parameters determined independently from the KMC simulations. This conventional approach is known to be unable to reproduce the correct island size distribution widely studied in Refs. 19 and 30 by introducing correlations between island and atom densities. Therefore we have limited our study to the behavior of the monomer and island densities and of the mean island size vs the terrace width.

The comparison of the results issued from KMC and RE is done in Sec. IV. Application of these data to Ag atoms

adsorbed on vicinal Pt surfaces allows us to validate the theoretical model.

II. KMC CALCULATIONS

A. The model

The usual deposition, diffusion, aggregation model[14] (DDA) is applied to the adsorption of atoms on a rectangular terrace of area ($L \times W$). The lattice geometry is chosen to be a square of unit side. Thus, L and W define the site number along the length and width, respectively. Atoms (or monomers) are generated randomly on single sites with a flux F (s^{-1}), and they diffuse from a site to an adjacent one with a diffusion coefficient D_1 (s^{-1}). When two monomers occupy adjacent sites, they form an irreversible, fixed, dimer, and so on, in order to produce growing motionless islands. We assume small coverages ($\theta \leqslant 0.1$) in order to avoid double layer growth. The influence of the finite size of the terrace is modeled as follows. Along the direction parallel to the step (along L), periodic conditions are applied, while the atoms moving to the upward and downward steps limiting the terrace obey asymmetric conditions. They irreversibly stick to the step foot and rebound on the wall (infinite barrier) mimicking the Schwoebel barrier at the step top. In this section, we consider aggregates as point objects, an assumption that will be commented in Sec. IV.

The number of initial available sites ($L \times W$) on the finite terrace is assumed to be constant and equal to 4×10^4, and the site number along the width is varied according to the series $W=5$, 8, 10, 16, 20, 25, 32, 40, and 50. We have also considered a larger value $W=200$, which corresponds to an infinitely wide terrace. In that case, periodic conditions have been applied on the two sides in order to mimic at best this infinite terrace situation. The diffusion coefficient D_1 per terrace area unit is fixed to 10^4 s^{-1}, a value which corresponds to a barrier of 1.6 T (meV) in the simplest site-site hopping model following the Arrhenius law, for a temperature T. The flux F has been varied from 5×10^{-6} to 10^4 monolayer s^{-1} in order to sample a wide set of F/D_1 values. Ten different runs have been performed for each terrace width to improve the statistics of our simulations. It may be noted that the variable F/D_1 is used (and not F and/or D_1, independently) since it is the usual way that scaling laws are displayed on infinite surfaces[14] but also because it has been verified that the results of simulation only depend on this ratio on finite size terraces.

B. Results

1. Island density

Figure 1 displays the behavior of the island density n, defined as the ratio of the island number over the number of terrace sites, as a function of the ratio F/D_1 using a decimal logarithmic scale, for the series of W values. For each calculated point, the standard deviation extracted from our statistics is given as vertical bars. This deviation, which remains very small at large fluxes increases significantly when the island density becomes small, i.e., when F strongly decreases. Preventing such an increase would require to increase the terrace size, and consequently the computational time which varies as the square of the number of sites.

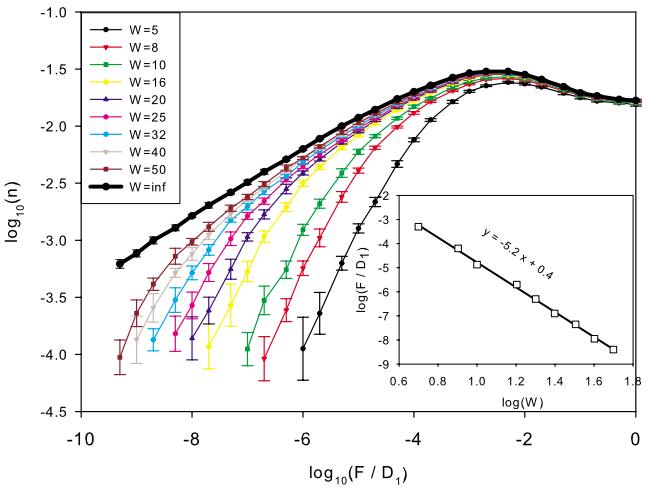

FIG. 1. (Color online) Behavior of the island density n as a function of the reduced flux F/D_1 in decimal logarithmic scale for the set of terrace widths. Error bars which correspond to data recorded from ten runs are also given. The bold curve describes the behavior on what is assumed to be an infinite terrace (see the text). The other curves from right to left characterize increasing terrace width W as mentioned in the figure. The inset displays the transition from infinite to finite (step capture) terrace growth process. Figures in color are available in the online version of the paper.

For the "infinite" terrace ($W=L=200$), the usual behavior is observed:[5,27] at very large values of the flux ($\ln F/D_1 > -1$), the percolation regime with a vanishing slope of the curve is dominant. When the flux decreases ($-2 \leqslant \ln F/D_1 \leqslant -1$), the diffusion favors the nucleation process and the slope of the curve increases. At smaller flux ($\ln F/D_1 < -3$), the diffusion prevails and island growth dominates with a slope equal to 0.33 ± 0.02. More precisely, the calculations lead to

$$n = A_n \left(\frac{F}{D_1} \right)^{1/3}, \tag{1}$$

where the constant $A_n \approx 0.8$ depends on the surface geometry, on the coverage and on the collision probability between monomers and islands (see Sec. III).

For the finite terraces, the behavior of the curves is not changed at large and intermediate fluxes when compared to the infinite case. However, at lower fluxes, competition proceeds between the island growth and the atom capture by the step. Indeed, at large diffusion, the density of islands is not sufficient to compete with the step attraction, and there is less available monomers to form islands. As a result, the slope of the curves dramatically changes, and the scaling law becomes

$$n = B_n \left(\frac{F}{D_1} \right), \tag{2}$$

where B_n is a function of the coverage, of the collision probabilities between the monomers and the islands, and of W

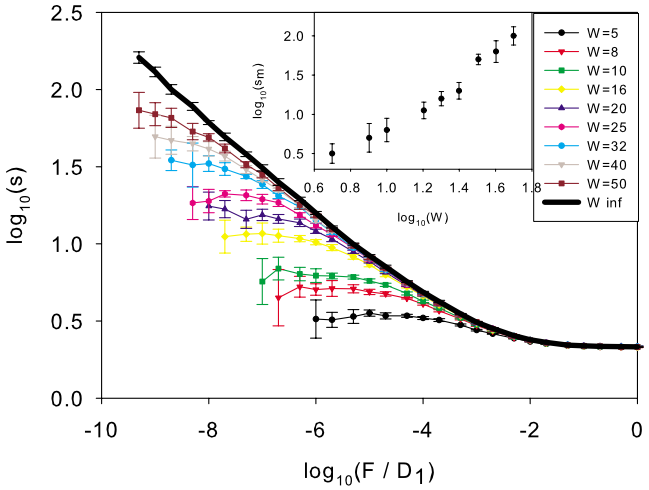

FIG. 2. (Color online) Mean size of islands s as a function of F/D_1 in decimal logarithmic scale, with vertical bars to estimate the standard deviation over ten runs. The bold curve corresponds to an infinite terrace. The other curves from bottom to top characterize increasing terrace width W. In the inset, we give the maximum size of islands as a function of the terrace width.

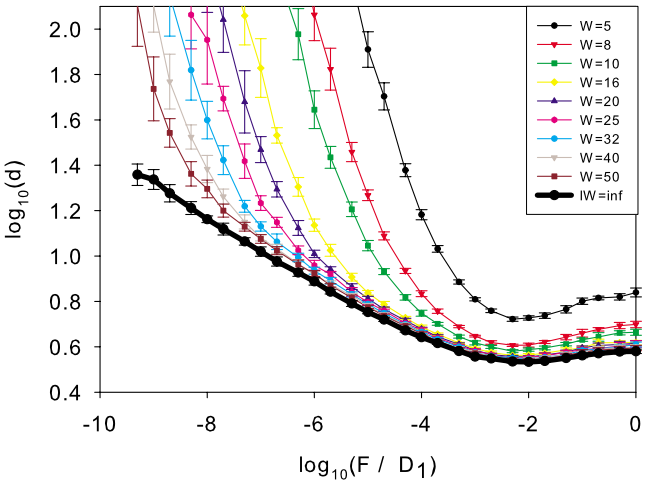

FIG. 3. (Color online) Mean reduced distance d between islands as a function of the reduced flux F/D_1 in decimal logarithmic scale for various terrace widths. Vertical bars show the standard deviation over ten runs. The bold curve corresponds to an infinite terrace. The other curves from left to right characterize decreasing terrace width W.

(see Secs. III and IV). The boundary between the two regimes with slopes 1/3 and 1 strongly depends on the terrace width. We can estimate the relation between F/D_1 where the transition occurs and W by determining the intersect of the asymptote of the infinite terrace curve with the asymptote of each curve corresponding to a given W value. This boundary drawn in decimal logarithmic scale in the inset of Fig. 1 can be fit to a straight line with a slope equal to −5.2, leading to the condition

$$\left(\frac{F}{D_1}\right)W^{5.2} = 2.5. \tag{3}$$

The change in the behavior of n vs F/D_1 [Eqs. (1) and (2)] displays some analogies with the model developed by Kandel[45] for a different situation where an energy barrier hinders the atom attachment to the island edges. In our case, this barrier does not exist, but the presence of the step foot acting as a sink tends to prevent the attachments to the island by decreasing the density of available atoms, especially when the terrace width is narrowed. According to the results of Ref. 45, values of the exponent in Eqs. (1) and (2) are smaller than 1 when the barrier is inefficient whereas they can be larger than 1 in the reverse situation, i.e., when the step becomes an efficient sink in our situation.

2. Island size

The behavior of the mean size s of islands as a function of F/D_1 in decimal logarithmic scale is shown in Fig. 2. At large flux, the value $s=2$ indicates the predominance of dimers in the percolation regime. When the flux decreases, s increases according to an asymptotic behavior obtained for the infinite terrace as

$$s = A_s\left(\frac{F}{D_1}\right)^{-1/3}, \tag{4}$$

where $A_s=0.13$ depends on the collision probability between monomers and islands and on the atom coverage.

However, for finite terraces, a breakdown of the slope, which dramatically depends on the terrace width, is observed, consistently with the change of island density (Fig. 1). For each width, a maximum size s_m for the islands is reached, according to the fact that the competition between the attachment to the step and the island growth favors the step sink when the terrace width decreases. Hence, this size s_m is an increasing function of W as shown in the inset in Fig. 2.

The behavior, which appears to be linear in decimal logarithmic scale for sufficiently large terraces ($W \geqslant 20$), tends to be inflected when W decreases. This behavior will be interpreted in Sec. III.

3. Mean distance between islands

The reduced mean distance d (where the lattice constant is 1) between nearest-neighbor islands vs the ratio F/D_1 is represented for each terrace width W in Fig. 3. At large flux, the final coverage is obtained before adatoms have had time to diffuse, so that the distance between island does not depend on the flux in the percolation regime. When the flux decreases on an infinite terrace, the monomer density decreases, thus the probability for a monomer to collide with another monomer decreases. As a consequence, nucleation is inhibited, the density of islands is reduced (Fig. 1) and the distance between islands increases (Fig. 3). On a finite terrace, the step attachment is responsible for a loss of monomers on the terrace, and the density of monomers decreases as the terrace width decreases. Then, the mean density of islands decreases (Fig. 1), and the mean distance between

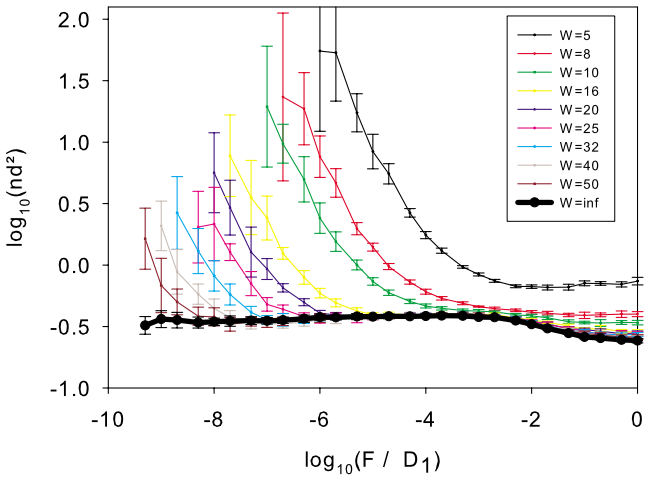

FIG. 4. (Color online) nd^2 vs F/D_1 in decimal logarithmic scale for the set of terrace widths. Error bars are given which correspond to the standard deviation over ten runs. The bold curve corresponds to the infinite terrace. Other curves shift toward the left when the terrace width W increases.

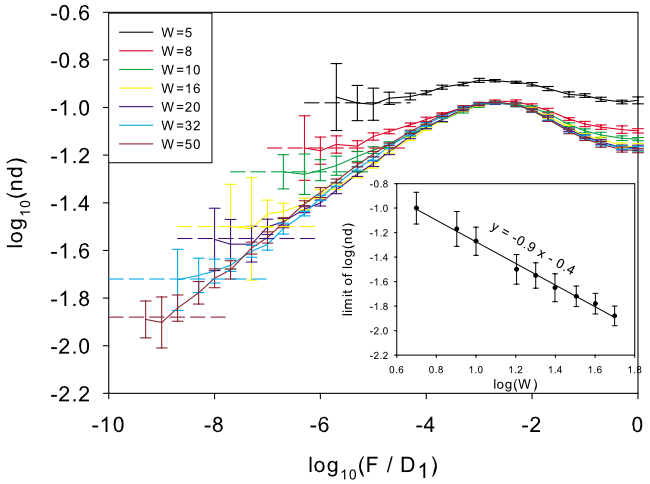

FIG. 5. (Color online) Evolution of the product nd vs the reduced flux F/D_1 in decimal logarithmic scale for the set of terrace widths. Error bars give the standard deviation obtained from ten runs. Curves slide toward the top as the terrace width W decreases. The inset displays the behavior of the limit of the quantity nd at low flux (shown by the broken lines on the curves) as a function of W. The points corresponding to $W=25$ and $W=40$ have been added.

islands increases (Fig. 3). To determine whether the island arrangement on the terrace is 1D, i.e., aligned along the step, or 2D, i.e., distributed on the terrace, we have drawn the behavior of the nd^2 (Fig. 4) and nd (Fig. 5) quantities as a function of F/D_1.

In Fig. 4, we see that nd^2 is nearly constant for the infinite terrace, indicating 2D distribution of islands as expected,[46] due to the fact that diffusion length is only limited by nucleation and percolation. This behavior remains valid for finite terraces if the terrace is sufficiently large or if the diffusion is low. More precisely, the limit of validity of this behavior follows the approximate formula

$$\frac{F}{D_1} \geqslant \frac{800}{W^{6.5}}. \tag{5}$$

Figure 5 shows that at low flux, the quantity nd tends to reach a plateau, depending on the terrace width, only. For still lower fluxes, the island number vanishes due to the step attachment, and the accuracy of the KMC results significantly decreases (hence the very large error bars shown in Fig. 5). This means that for narrow terrace or fast diffusion, islands are aligned on the terrace along the step, because the diffusion length is then limited by the presence of the step. This behavior could look surprising since diffusion is assumed to be isotropic through the single D_1 quantity. In fact, this latter becomes anisotropic due to the terrace anisotropy. Moving perpendicular to the step means to be sticked whereas diffusion parallel to the step allows one to meet other monomer or existing islands, that is, to nucleate or to grow. This behavior remains valid when the following condition is fulfilled:

$$\frac{F}{D_1} \leqslant \frac{0.05}{W^{4.4}}. \tag{6}$$

Within this limit, the mean distance between islands along the step depends on the island density and the terrace width according to the law

$$d_m = \frac{0.4}{nW^{0.9}} \tag{7}$$

deduced from the line drawn in the inset of Fig. 5. If the islands were uniformly distributed along the step, one would expect $d_m=1/nW$. The coefficient 0.4 in Eq. (7) quantifies the dispersion of this distribution.

4. Step attachment

To estimate the reduced number of atoms which are sticked at the step foot, we have drawn, in Fig. 6, the ratio n_s of monomers irreversibly attached to the step over the number of sites on the terrace vs F/D_1. At large flux, n_s is vanishingly small, due to the reduced diffusion. When the flux decreases, the attachment is more favored for narrow terraces, and at still smaller flux, most of the atoms are close to the step, indicating a saturation in the curves. Another way to interpret these data is to consider the step coating. At large flux, the step does not practically move (no step flow) due to atom attachment, while at low flux, the coating follows the coverage value. In this step flow regime, one additional row occurs on a $W=10$ terrace while two can occur for $W=20$.

C. General trends of growth on finite terraces

To conclude this section, we have shown the influence of atom confinement by terrace width and found asymptotic behaviors with their range of validity. At large flux, the asymptotic behavior of the island density n follows the formula $n=0.016$ whatever the terrace size. In contrast, at small

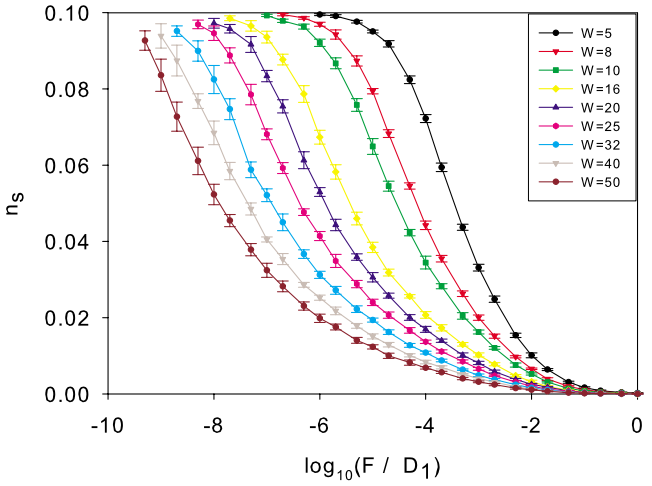

FIG. 6. (Color online) Behavior of the number of atoms attached to the step reduced by the total number of sites vs the decimal logarithm of the reduced flux F/D_1. Error bars correspond to the standard deviation over ten independent runs. The curves shift toward the left as the terrace width W increases.

flux, the island density changes with the terrace width, from a law $n \propto (F/D_1)^{1/3}$ which is consistent with the infinite terrace behavior, to a law $n \propto (F/D_1)$. The values of F/D_1 corresponding to the slope breakdown decrease as the inverse of the terrace width, according to the full line behavior drawn in Fig. 7. The island size s displays a behavior which is consistent with that of n. At large flux, one has $s=2$, indicating the formation of dimers, while at small flux, the law $s \propto (F/D_1)^{-1/3}$ for infinite terrace changes to an asymptotic value that increases with the terrace size.

The behavior of the mean distance between islands allows us to define two regions shown in Fig. 7. The region at sufficiently large flux and/or wide terrace describes the terrace regime with $d^2 \propto 1/n$ (broken-dotted line), whereas the region at small flux and/or narrow terrace corresponds to the growth at step edges with $d \propto 1/n$ (dotted line). The terrace regime obeys the condition given by Eq. (5) and the step one which is directly connected to the influence of atom confinement follows Eq. (6).

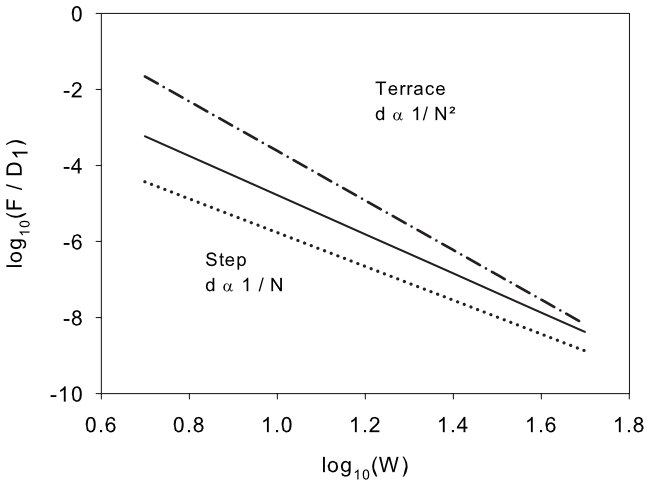

FIG. 7. Behavior of the reduced flux F/D_1 vs the terrace width W in decimal logarithmic scale. The two broken lines define the asymptotic limits of the terrace and step regimes as defined by Eqs. (5) and (6). The full line defines the transition given by Eq. (3).

III. RE APPROACH

At this step, our KMC results look quite convincing concerning the influence of surface confinement on the growth process. However, we have extracted power laws and prefactors [Eqs. (1)–(7)] which could be quantitatively understood on the basis of rate equations. Moreover, some assumptions made in our simulations could be justified using the RE approach.

A. The model

The time variation of the mean density of monomers (in monolayer per second unit) on a terrace is approached by the equation

$$\frac{dn_1}{dt} = F(1 - Ft) - 2k_1 D_1 n_1^2 - kD_1 n_1 n - 4Fn - 8Fn_1 - k_w D_1 n_1, \tag{8}$$

where the first term on the right-hand side (RHS) of Eq. (8) creates the monomers on the terrace and the second and third terms describe the loss of monomers that nucleate or participate to the island growth, respectively. The fourth and fifth terms correspond to direct impingement of deposited monomers onto monomers or islands. Therefore, in our situation, the fourth term characterizes the loss of monomers that stick to one among the four available sites around a point island (for a square lattice) while the fifth one describes the monomer loss due to the sticking close to a monomer (two monomers are then lost). The last term takes into account the monomer attachment to the step, by assuming that this irreversible sticking is proportional, through k_w, to the density of monomers and to the diffusion coefficient D_1 on the terrace. The parameters k and k_1 can be related to the efficiency of monomer-island and monomer-monomer collisions in the nucleation process, respectively. The time evolution of the island density is approached by the equation

$$\frac{dn}{dt} = k_1 D_1 n_1^2 + 4Fn_1, \tag{9}$$

where the RHS terms characterize the formation of an island due to monomer-monomer nucleation and to percolation, respectively. Note that, compared to Eq. (8), a factor 2 disappears due to the fact that these two processes create only one island, while two monomers disappear.

We add an equation describing the mean island size s defined as the ratio of the density n_i of atoms in the islands over the density of islands n. The density n_i follows the rate equation

$$\frac{dn_i}{dt} = 2k_1 D_1 n_1^2 + kD_1 n_1 n + 4Fn + 8Fn_1 \tag{10}$$

and the time behavior of $s(t)$ can be obtained from the knowledge of n_i and n. Finally, the density of atoms attached to the step can be quantified using the equation

$$\frac{dn_s}{dt} = k_w D_1 n_1. \tag{11}$$

Note that Eqs. (8) and (9) form the basis of the RE approach since they are intrinsically coupled, while Eqs. (10) and (11) only serve to define observables which depend on the data extracted from the previous Eqs. (8) and (9).

B. Asymptotic behavior of the solutions of the RE

An asymptotic study of the n and s behaviors shows that, at large flux, simple relations are obtained, which do not depend on the parameters introduced in the rate equations. They are written[14,47] as

$$n \approx 2\theta^2 \tag{12}$$

and

$$s \approx 2 \tag{13}$$

indicating the dominant formation of dimers in the percolation regime.

On the contrary, at small flux, the asymptotic behavior of n and s varies according to the terrace width. For an infinite terrace, we obtain

$$n \approx \left(\frac{3k_1\theta}{k^2}\right)^{1/3}\left(\frac{F}{D_1}\right)^{1/3} \tag{14}$$

$$s \approx \frac{k^2\theta^2}{3k_1^2}\left(\frac{F}{D_1}\right)^{-1/3} \tag{15}$$

while for a finite one with width W, the dependence of n and s becomes

$$n \approx \frac{k_1\theta}{k_w^2}\frac{F}{D_1}, \tag{16}$$

$$s \approx \frac{k\theta}{2k_w} + 1. \tag{17}$$

Equations (14)–(17) follow the same scaling laws already obtained in Sec. II with KMC simulations. This also leads to the expression of the coefficients $A_n=(3k_1\theta/k^2)^{1/3}$, $A_s=k^2\theta^2/3k_1^2$, and $B_n=k_1\theta/k_w^2$, defined in Eqs. (1), (4), and (2), respectively, showing that these three coefficients depend on the efficiencies of monomer-monomer, monomer-island, and monomer-step collisions, on the coverage, and on the geometry of the system, via k_1 and k. On the contrary, the exponents of F/D_1 do not depend on these quantities and their values are totally consistent with the KMC data. Three parameters k_1, k, and k_w should thus be estimated to allow for a direct comparison of RE results with KMC data. The goal here is to determine these parameters in a self-consistent way, i.e., independently of the KMC data.

C. Determination of parameters k and k_1

We can estimate k_1 and k independently using subsidiary simple simulations. To determine k_1, we calculate the number of collisions between four monomers deposited on a (200×200) square surface. The monomer density is thus very small. 10^7 random diffusions are then allowed for the monomers, with no possible aggregation (i.e., when two monomers collide, they are randomly redeposited on the surface). When we compare the number of collisions between monomers and the number of diffusions to estimate k_1, we can see that this value is nearly constant and equal to 0.45 ± 0.03 at low monomer density, from ten independent calculations. This situation corresponds to the conditions of low flux regime where the effect of the step is dominant. Indeed, the k_1 value significantly increases with the monomer density.

The same kind of trivial simulations are performed to estimate the efficiency of collisions k between a monomer and a fixed point island, which is in fact the diffusion efficiency of a single monomer. On the same (200×200) surface, we calculate the mean number of visited sites after 10^2 random diffusions of a single monomer. The value found is $k=0.49\pm0.02$, after 100 independent calculations.

D. Determination of the parameter k_w

An analytical model allows us to determine the distribution of monomers in the various rows parallel to the step, where the row labeled zero corresponds to the step sticking, and the other rows are labeled from 1 to W, depending on their proximity to the step. We assume that the monomers are independent and that no island is present on the surface. The monomer density m_r on the rth row is given by the equation

$$\frac{dm_r}{dt} = F + Dm_{r-1} - 2Dm_r + Dm_{r+1}. \tag{18}$$

In this equation, D (in s^{-1}) defines the probability for a monomer to jump from a row to the nearest neighbor one. The first, second and fourth terms describe the gain of monomers due to direct deposition and to diffusion from the $(r-1)$th and $(r+1)$th rows. The third one is the loss of monomers in the rth row due to their diffusion toward the $(r-1)$th and $(r+1)$th rows. A particular behavior for the first and last rows, due to the asymmetric boundary conditions, is given by

$$\frac{dm_1}{dt} = F - 2Dm_1 + Dm_2,$$

$$\frac{dm_W}{dt} = F + Dm_{W-1} - Dm_W. \tag{19}$$

A numerical solution is required for the complete range of fluxes. Equations (18) and (19) have been solved numerically for $W=20$, $D=D_1/4$ for the square lattice and F ranging from 10^{-2} to 10^3. Results are presented in Fig. 8(a), which shows that the monomer density is distributed quasiuniformly at large flux on the surface. When the flux decreases,

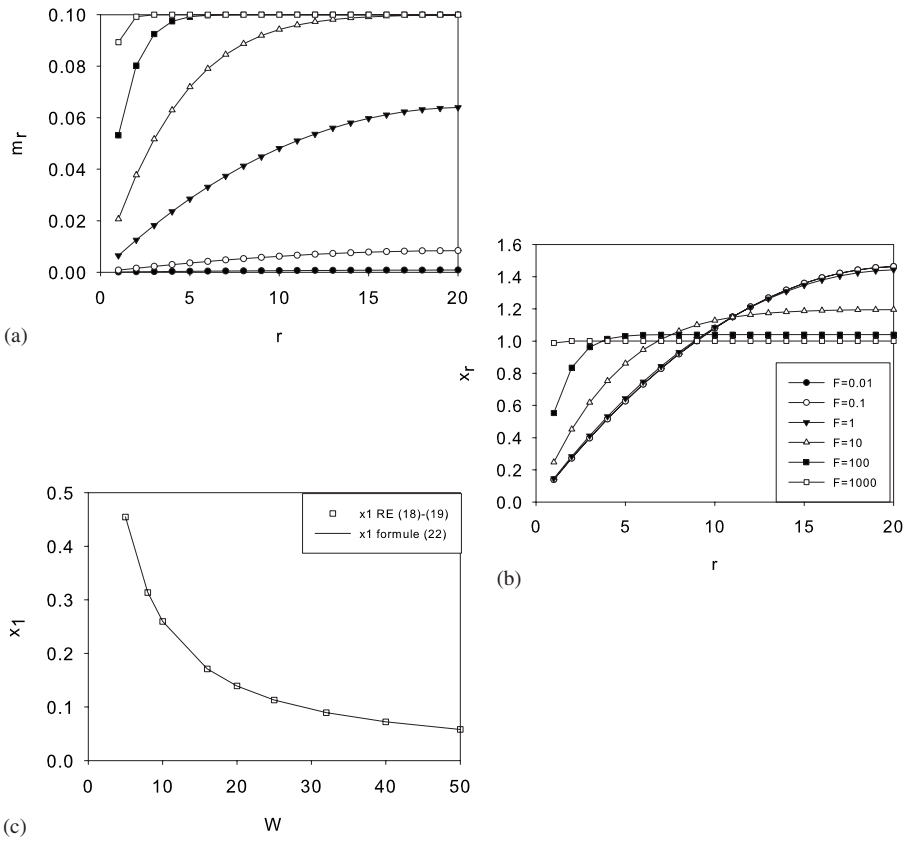

FIG. 8. (a) Monomer density m_r on the rth row vs the row number r for different fluxes. (b) Behavior of the ratio x_r of monomers in the rth row vs r for the same set of fluxes. (c) Comparison of numerical results [squares, Eqs. (18) and (19)] with analytical model [curve, Eq. (22)] for the ratio x_1 of monomers in the first row as a function of the terrace width W.

this density decreases on the rows close to the side ($r=0$) since the diffusion favors the monomer sticking to the step. The distribution of monomers increases from the first row to the last one due to this asymmetric sticking.

In Fig. 8(b), the ratio $x_r = m_r / \Sigma_{r'=1}^{W} m_{r'}$ of monomers in the rth row is drawn as a function of the row number from $r=1$ to 20 for the same range of flux values. We see that, at flux less than or equal to $F \approx 1$, the x_r curve does not evolve, indicating an asymptotic behavior. Using this remark, an analytical model can be obtained at small flux by disregarding transient regimes. Within this assumption, the density m_r of monomers in the rth row can be calculated as

$$m_r = \sum_{k=0}^{r-1} (W-k)\left(\frac{F}{D}\right) = \left[r\left(W+\frac{1}{2}\right) - \frac{r^2}{2} \right]\left(\frac{F}{D}\right). \quad (20)$$

From Eq. (20), we can easily calculate the ratio x_r of monomers in the rth row as

$$x_r = \frac{6}{(W+1)(2W+1)}\left[r\left(W+\frac{1}{2}\right) - \frac{r^2}{2} \right] \quad (21)$$

which gives for the first row

$$x_1 = \frac{6W}{(W+1)(2W+1)}. \quad (22)$$

Note that Eqs. (21) and (22) depend on the terrace width, through W but not on D and F.

Figure 8(c) shows the behavior of x_1 vs W, the squares correspond to the calculations at small flux using Eqs. (18) and (19), while the curve is drawn from Eq. (22). The agreement is excellent.

If the distribution of monomers was uniform in the rows, the number of monomers in the first row would be N_1/W for a given number N_1 of monomers on the surface. Due to the step asymmetry, this number is $x_1 N_1 / W$. Each monomer moves toward the step every $D_1/4$ times per second (for a square lattice) and it becomes irreversibly attached to this step when located in the first row. The loss of monomers by step attachment is then given by

$$\frac{dn_1}{dt} = -x_1 \frac{D_1}{4W} n_1. \quad (23)$$

The comparison with the loss term in Eq. (8) finally gives an analytical expression for k_w as

$$k_w = \frac{x_1}{4W} = \frac{3}{2}\frac{1}{(W+1)(2W+1)}. \quad (24)$$

This equation shows that k_w varies roughly as W^{-2}.

E. Results

Once the three parameters in RE approach have been estimated independently, one can use Eqs. (8)–(11) to draw the behavior of the island density n and size s, and the reduced number n_s of atoms attached to the step as a function of F/D_1, in complete analogy with the KMC data. The curves are given in Figs. 9, 10, and 11, respectively, using the same

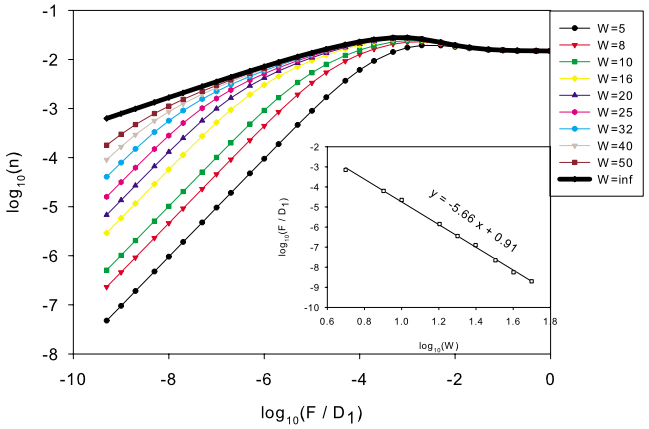

FIG. 9. (Color online) Behavior of the island density n vs the reduced flux F/D_1 for various terrace widths obtained from the RE approach. The bold curve represents the case of an infinite terrace. Other curves from right to left characterize increasing terrace width W. The inset displays the transition from infinite to finite terrace growth process.

scheme as in Figs. 1, 2, and 6. The influence of atom confinement by step is clearly observed in Figs. 9 and 10, with asymptotic behaviors at small and large fluxes. The inset in Fig. 9 displays the linear behavior of the boundary between the infinite and finite terrace and the inset in Fig. 10 exhibits the nonlinear dependence of the maximum island size s_m at small flux.

IV. DISCUSSION

A. Comparison of RE and KMC results

We compare the three quantities, mean island density and size and reduced number of atoms attached to the step, which have been calculated as functions of the ratio flux over diffusion constant of monomer using KMC simulations and rate

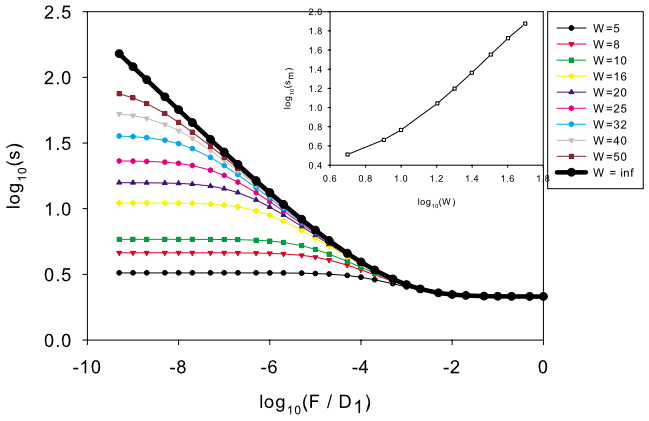

FIG. 10. (Color online) Behavior of the island size s vs F/D_1 for various terrace widths obtained from RE approach. The bold curve corresponds to an infinite terrace. The other curves shift toward the bottom as the terrace width W decreases. In the insert is drawn the maximum size of islands as a function of W.

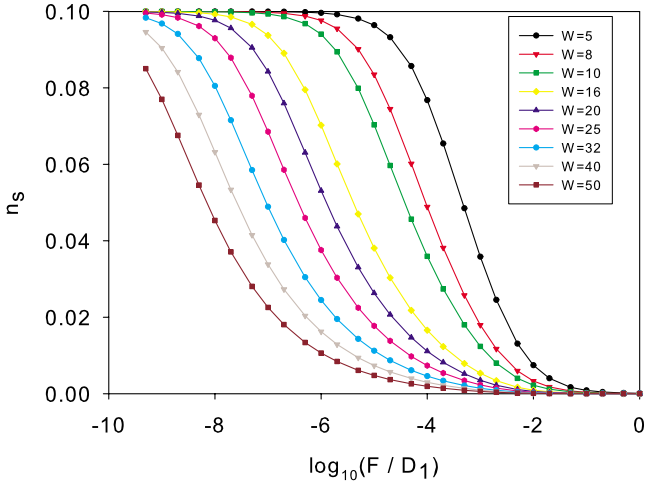

FIG. 11. (Color online) Behavior of the reduced number of atoms attached to the step vs F/D_1 for different widths, obtained from RE approach. Curves from left to right correspond to an increase of the terrace width W.

equations model. Within the assumption of point island and irreversible aggregation, the influence of atom confinement on terraces with different widths W has been shown to be dominant at small flux in the KMC simulations. Within the same hypotheses, the RE approach with three parameters, the collisional efficiency between monomers, between monomers and islands and the attachment efficiency of the monomers to the step, can be self-consistently studied, since these parameters have been determined independently of the KMC data. The agreement between the KMC and RE results is excellent at small flux. The shape and slopes of the curves n, s, and n_s vs F/D_1 are very similar, especially in their asymptotic part. Note, however, a slight shift of the maximum for the $n(F/D_1)$ curves in RE approach at intermediate flux. This can be explained by the fact that the values of k_1 and k depend in fact on the monomer and island densities, and even on W, instead of being constant, as considered here. This dependency, which is negligible at small flux, comes to play a role at intermediate flux.

The agreement between KMC and RE results can also be viewed through the behavior of k_w vs W. Indeed, from the asymptotic behavior of the curves $n(F/D_1)$ in Fig. 1, we can estimate k_w for the various terrace widths using Eq. (16). Figure 12 displays the set of points (circles) obtained from this estimate. It can be satisfactorily compared with the curve drawn from the analytical expression of $k_w(W)$ given in Eq. (24) from an asymptotic study of the RE. This comparison allows us to validate the simple models used to determine k_1, k, and k_w in the RE approach.

Moreover, from Eq. (17), the maximum size s_m can be estimated at small flux as a function of the terrace width. In Fig. 13, we compare s_m calculated from KMC data (squares), the broken curve determined by solving Eqs. (8)–(11) and the full curve drawn from the asymptotic model [Eq. (17)]. The agreement demonstrates here again that relatively simple asymptotic expressions can accurately describe the behavior obtained from more complete calculations and from more time expensive simulations.

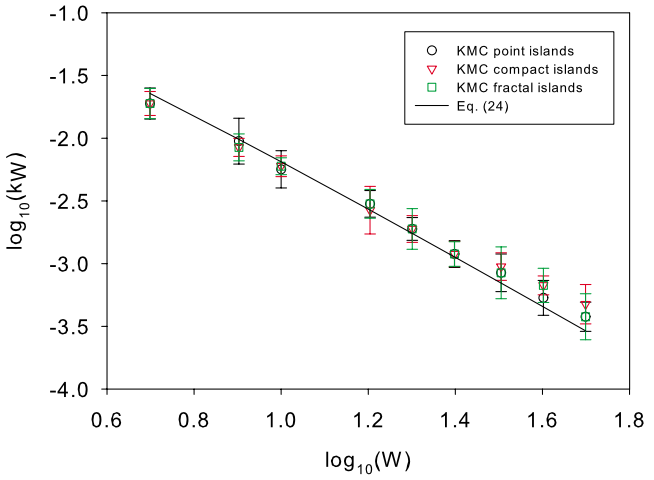

FIG. 12. (Color online) Behavior of the step capture efficiency k_w vs the terrace width W in decimal logarithmic scale. The line is drawn from the analytical expression (24) and the symbols correspond to KMC data by assuming point (circles), compact (triangles), and fractal (squares) islands.

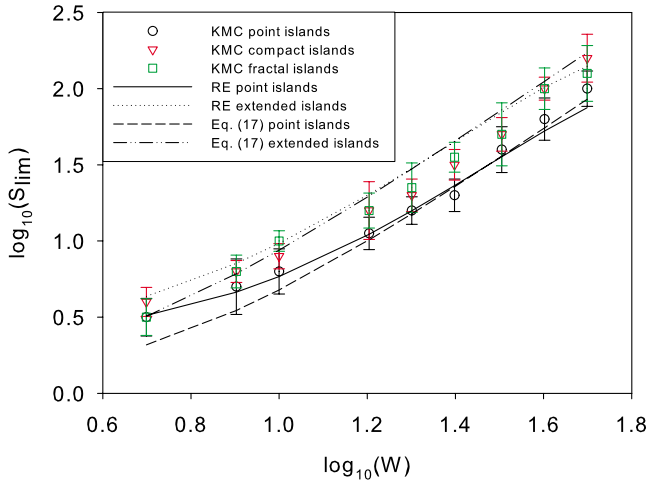

FIG. 13. (Color online) Comparison of the limit value of the mean size s_m of islands at very small flux vs the terrace width W from various methods.

B. Toward real systems: Compact or fractal islands

Two main assumptions have been done in the present KMC simulations: The irreversible sticking of monomers to islands and to the step, and the point structure of the islands. One can, however, wonder if the RE approach in Sec. III remains valid when these assumptions are removed. The influence of reversible sticking on the results will be discussed in detail, in a forthcoming paper.

We have considered the case of extended, compact, or fractal islands which can form on the terrace depending on the experimental conditions. KMC simulations have been performed by keeping the same characteristics as in Sec. II, but releasing the stress on the point islands. The results (not shown) on the behavior of n, s, and n_s vs F/D_1 do not appreciably change the shape of the curves. In particular the exponents of F/D_1 for the infinite and finite terraces remain the same, although the coefficients A_n, B_n, and A_s are modified. (A_n=0.50/0.45 and A_s=0.20/0.22 for compact/fractal islands.)

When the model is generalized to extended islands in the RE approach, the value of the k parameter has to be modified to account for the influence of such an extension on the collision probability between monomers and islands, while the collisional efficiency k_1 between monomers is not changed. The value k=1 instead of 0.49 gives a good agreement between the KMC curves and the RE results, as shown in Fig. 12 for the dependence of k_w vs W and Fig. 13 for the behavior of the maximum island size s_m. Such an increase of k by a factor 2 when compared to the point island model can be understood as an increased efficiency of the colliding process between monomers and extended islands.[23] We could think that k should be *a priori* different for compact and fractal island shapes.[29,30] Indeed some terms in Eqs. (8) and (9) should be changed, especially the factor 4 which becomes inadequate to describe the site multiplicity for a monomer around an extended island. However, this term, which corresponds to percolation, is very small for a description of the island growth at small flux, and thus for the study of the influence of the confinement on the surface. In fact, it seems that the details of the island shape do not have a significant influence on the collisional efficiency parameter k, at least within the accuracy of our approach.

C. Example of a real system: Ag adsorbed on vicinal surfaces of Pt

To end this paper, we have studied a real system, namely the growth of Ag atoms on vicinal surfaces of platinum with terrace width W=6,8,18 and on an infinite terrace. Indeed the previous results (KMC and RE) do not depend on the atom and surface characteristics. We want to show here that they should apply to any system, provided the hypothesis of small flux is assumed.

KMC simulations based on semiempirical description of metal-metal interactions (Ag-Ag and Ag-Pt pairs), previously used[43] to interpret experiments devoted to the formation of silver wires at the steps of the vicinal Pt(997) surface with W=6, have been extended to variable terrace widths. The growth model includes the atom deposition, diffusion, and reversible aggregation on islands and steps (DDA model), described within the Arrhenius law by a set of processes characterized by energy barriers issued from the knowledge of the metal-metal interactions.[43] The temperature is chosen to be equal to 100 K. The main difference with previous KMC simulations is that we take into account the real interactions so that the diffusion looks very anisotropic.

The RE approach (Sec. III) has been applied to this physical system by adapting Eqs. (8) and (9). The percolation terms have been corrected to account for the triangular symmetry of the Pt(111) surface. The factor 4 has been replaced by 6. The value k=1 obtained for the extended island approach on a square lattice is kept the same, assuming that it does not depend on the surface geometry. For k_1, the value obtained for the square lattice is increased by a factor 3/2 to

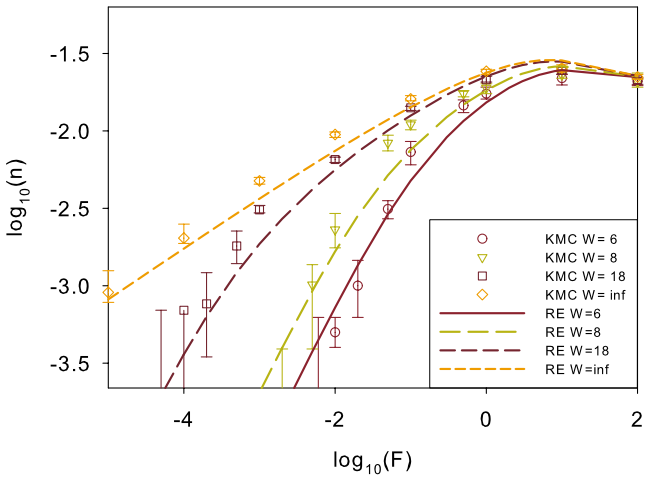

FIG. 14. (Color online) Behavior of the island density n as a function of the deposition flux F in decimal logarithmic scale for the Ag/Pt system, as calculated from a DDA growth model (see the text). The curves correspond to different terrace widths, including the infinite terrace (bold curve).

account for the available sites around a monomer in a triangular geometry (6 instead of 4). The value of k_w is not changed. The value of the diffusion coefficient cannot be easily determined since several processes are implied in the atomic approach of KMC. Therefore, we have retained a value $D_1=4\times10^3$ s^{-1}, which corresponds to an activation barrier equal to an average value over the efficient processes, i.e., 177 meV.

The results shown in Fig. 14 give the behavior of the island density n as a function of F in decimal logarithmic scale to be directly compared with Figs. 1 and 9. The points correspond to KMC data, whereas the curves are issued from RE approach. The confinement influence at small flux is clearly observed, with a breakdown of the slopes that depends on the terrace width and a behavior with F/D_1 which scales with the expected critical exponent 1 [Eq. (3)]. The agreement is quantitatively correct since the main characteristics of the growth mechanisms on vicinal surfaces discussed in Secs. II and III are recovered.

V. CONCLUSION

We have developed both KMC simulations and RE approach to understand the influence of atom confinement in the growth process on vicinal surfaces with various widths. In these two methods, the evaporation, exchange and reversibility in the aggregation have been disregarded. Most of the results have been obtained by considering a point-island model. The simplicity of this model has been exploited in the RE approach by building self-consistent equations containing a limited number (3) of parameters determined independently from the KMC data. Asymptotic behaviors of island density and size vs the ratio "flux over diffusion coefficient of monomers," and especially the breakdown in these curves due to the step capture found in KMC data have been well interpreted with the RE approach. Extension of these calculations to extended islands requires to change the value of the parameter describing the efficiency of the monomer-island collisions in the RE approach, only. This change is sufficient to recover the data obtained from KMC, as shown by the consistent behavior of the parameter describing the capture of the atoms by the step for various terrace widths, whatever the point/compact/fractal-island model used. Finally, the general results obtained from the two approaches (KMC and RE) are shown to satisfactorily apply to specific calculations carried out for the Ag/Pt system. In a forthcoming paper, we will explore the deviations from these results by investigating the Ag/Pt system in the whole temperature, flux, and coverage ranges.

[1] H. Brune, Surf. Sci. Rep. **31**, 121 (1998).
[2] T. A. Witten and L. M. Sander, Phys. Rev. Lett. **47**, 1400 (1981).
[3] T. A. Witten and L. M. Sander, Phys. Rev. B **27**, 5686 (1983).
[4] P. Meakin, Phys. Rev. Lett. **51**, 1119 (1983).
[5] J. A. Venables, G. D. T. Spiller, and M. Hanbücken, Rep. Prog. Phys. **47**, 399 (1984).
[6] H. J. Herrmann, Phys. Rep. **136**, 153 (1986).
[7] J. A. Venables, Phys. Rev. B **36**, 4153 (1987).
[8] G. S. Bales and A. Zangwill, Phys. Rev. B **41**, 5500 (1990).
[9] V. Fuenzalida, Phys. Rev. B **44**, 10835 (1991).
[10] M. C. Bartelt and J. W. Evans, Phys. Rev. B **46**, 12 675 (1992).
[11] G. S. Bales and D. C. Chrzan, Phys. Rev. B **50**, 6057 (1994).
[12] J. G. Amar, F. Family, and P. M. Lam, Phys. Rev. B **50**, 8781 (1994).
[13] J. A. Venables, Surf. Sci. **299/300**, 798 (1994).
[14] P. Jensen, A. L. Barabási, H. Larralde, S. Havlin, and H. E. Stanley, Phys. Rev. B **50**, 15316 (1994).
[15] J. W. Evans and M. C. Bartelt, J. Vac. Sci. Technol. A **12**, 1800 (1994).
[16] C. Ratsch, A. Zangwill, P. Smilauer, and D. D. Vvedensky, Phys. Rev. Lett. **72**, 3194 (1994).
[17] J. G. Amar and F. Family, Phys. Rev. Lett. **74**, 2066 (1995).
[18] M. C. Bartelt and J. W. Evans, Surf. Sci. **344**, L1193 (1995).
[19] M. C. Bartelt and J. W. Evans, Phys. Rev. B **54**, R17 359 (1996).
[20] J. G. Amar and F. Family, Thin Solid Films **272**, 208 (1996).
[21] J. A. Blackman and P. A. Mulheran, Phys. Rev. B **54**, 11 681 (1996).
[22] P. A. Mulheran and J. A. Blackman, Surf. Sci. **376**, 403 (1997).
[23] P. Jensen, H. Larralde, and A. Pimpinelli, Phys. Rev. B **55**, 2556 (1997).
[24] N. Combe and P. Jensen, Phys. Rev. B **57**, 15 553 (1998).
[25] M. N. Popescu, J. G. Amar, and F. Family, Phys. Rev. B **58**, 1613 (1998).
[26] H. Brune, G. S. Bales, J. Jacobsen, C. Boragno, and K. Kern, Phys. Rev. B **60**, 5991 (1999).
[27] P. Jensen, Rev. Mod. Phys. **71**, 1695 (1999).
[28] D. D. Vvedensky, Phys. Rev. B **62**, 15435 (2000).
[29] M. N. Popescu, J. G. Amar, and F. Family, Phys. Rev. B **64**,

205404 (2001).
[30] J. G. Amar, M. N. Popescu, and F. Family, Phys. Rev. Lett. **86**, 3092 (2001).
[31] J. G. Amar, M. N. Popescu, and F. Family, Surf. Sci. **491**, 239 (2001).
[32] J. W. Evans and M. C. Bartelt, Phys. Rev. B **63**, 235408 (2001).
[33] J. W. Evans and M. C. Bartelt, Phys. Rev. B **66**, 235410 (2002).
[34] J. G. Amar and M. N. Popescu, Phys. Rev. B **69**, 033401 (2004).
[35] F. Shi, Y. Shim, and J. G. Amar, Phys. Rev. B **71**, 245411 (2005).
[36] F. Shi, Y. Shim, and J. G. Amar, Phys. Rev. E **74**, 021606 (2006).
[37] D. Kandel and E. Kaxiras, Phys. Rev. Lett. **75**, 2742 (1995).
[38] D. Kandel and E. Kaxiras, Solid State Phys. **54**, 219 (2000).
[39] V. Cherepanov, S. Filimonov, J. Mysliveček, and B. Voigtländer, Phys. Rev. B **70**, 085401 (2004).
[40] D. Wang, Z. Ding, and X. Sun, Phys. Rev. B **72**, 115419 (2005).
[41] A. Ballestad and T. Tiedje, Phys. Rev. B **74**, 153405 (2006).
[42] A. Pimpinelli, V. Tonchev, A. Videcoq, and M. Vladimirova, Phys. Rev. Lett. **88**, 206103 (2002).
[43] F. Picaud, C. Ramseyer, C. Girardet, and P. Jensen, Phys. Rev. B **61**, 16154 (2000).
[44] C. Girardet, C. Ramseyer, and F. Picaud, Phys. Scr. **T68**, C104 (2003).
[45] D. Kandel, Phys. Rev. Lett. **78**, 499 (1997).
[46] J. Villain and A. Pimpinelli, *Physique de la Croissance Cristalline* (Eyrolles, Paris, 1995).
[47] D. Stauffer and A. Aharony, *Introduction to Percolation Theory* (Taylor and Francis, London, 1992).